Journal of Systems Engineering and Electronics
Vol. PP, No. 99, December 2023, pp.1 – 10

Ship recognition based on HRRP via multi-scale sparse preserving method

YANG Xueling[1,2,3], ZHANG Gong[1,2,*], and SONG Hu[3]

1. College of Electronic and Information Engineering, Nanjing University of Aeronautics and Astronautics, Nanjing 210016, China;
2. Key Lab of Radar Imaging and Microwave Photonics, Ministry of Education, Nanjing 210016, China;
3. Nanjing Marine Radar Institute, Nanjing 210016, China

Abstract: In order to extract the richer feature information of ship targets from sea clutter, and address the high dimensional data problem, a method termed as multi-scale fusion kernel sparse preserving projection (MSFKSPP) based on the maximum margin criterion (MMC) is proposed for recognizing the class of ship targets utilizing the high-resolution range profile (HRRP). Multi-scale fusion is introduced to capture the local and detailed information in small-scale features, and the global and contour information in large-scale features, offering help to extract the edge information from sea clutter and further improving the target recognition accuracy. The proposed method can maximally preserve the multi-scale fusion sparse of data and maximize the class separability in the reduced dimensionality by reproducing kernel Hilbert space. Experimental results on the measured radar data show that the proposed method can effectively extract the features of ship target from sea clutter, further reduce the feature dimensionality, and improve target recognition performance.

Keywords: ship target recognition, high-resolution range profile (HRRP), multi-scale fusion kernel sparse preserving projection (MSFKSPP), feature extraction, dimensionality reduction.

DOI: 10.23919/JSEE.2023.000136

1. Introduction

High-resolution range profile (HRRP) can imply the detailed physical structure characteristics of the target, such as the scatterer distribution, the target size, and other abundant information [1]. Recently, it has been widely used in the radar automatic target recognition (RATR). At present, the recognition technology based on HRRP is mainly used in air targets [2−4]. According to most of the research results obtained in the environment of Gaussian white noise, the HRRPs of air targets are mainly affected by noise. Different from air targets, the HRRPs of ship targets are influenced by the superimposed echo reflected by sea clutter [5]. The sea clutter is related to many factors, usually showing the obvious non-stationary and non-Gaussian characteristics. The existence of sea clutter leads to the changes in the HRRP structure of the ship target.

Compared with air targets, the dynamic range of ship target length is larger [6]. For the ship target, in addition to the position and amplitude information of the scattering point, the edge information is also very important [7]. The edge points can enhance HRRP samples' separability which consequently lead to the improvement of classification performance. In this issue, feature extraction of the ship target from the sea clutter is an essential procedure for robust target recognition. In fact, compared with sea clutter, the target only occupies a small part of range units in a wideband data gate, causing the dimension to increase and difficulties to discover knowledge from HRRP. Therefore, it is necessary to reduce the dimensionality of samples.

To address the problem of dealing with high dimensional data, most dimensionality reduction methods have commonly been used as principled ways. Several dimensionality reduction methods were proposed to tackle this problem and have been used in HRRP RATR, such as principal component analysis (PCA) [8], linear discriminant analysis (LDA) [9], neighborhood preserving projection (NPP) [10], and sparse preserving projection (SPP) [11]. However, most of the above methods are linear and may encounter some problems when processing nonlinear data. The kernel trick is a common technique for dealing with nonlinear data [12−14], which extends linear methods to nonlinear methods. Hence, the kernel trick is

Manuscript received June 13, 2022.
*Corresponding author.
This work was supported by the National Natural Science Foundation of China (62271255; 61871218), the Fundamental Research Funds for the Central University (3082019NC2019002), the Aeronautical Science Foundation (ASFC-201920007002), and the Program of Remote Sensing Intelligent Monitoring and Emergency Services for Regional Security Elements.

investigated to map the nonlinear and inseparable data into a high dimensional feature space, in which data is easily grouped together and is linearly separable. Inspired by the fact above, Liu et al. [15] introduced a kernel joint discriminant analysis (KJDA) method which utilizes more potential information captured from global and local criterion of input data in kernel feature space. Zhou et al. [16] proposed an orthogonal kernel projecting plane (OKPP) algorithm for radar target recognition. Although kernel trick may be more conveniently used in practice, it still suffers from the problem of information loss of ship target HRRP. For instance, the above feature extraction methods mainly focus on the position and amplitude information of the strong scatters. Nevertheless, the edge information presented by weak scatters is often neglected.

To extract edge information from HRRP, some researchers have achieved certain results. In [17], a sparse recovery via iterative minimization method was proposed to estimate the complex HRRPs of ships. However, it is assumed that the HRRP of the target is independent of sea clutter. Liu et al. [18] extended the target range profile features from single scale to multi-scale. The edge points of range profiles were extracted and a novel multi-scale target classification method was proposed. The multi-scale structure is helpful for recovering information loss better. However, independent recognition based on features at different scales leads to the isolation of recognition information between different scales and costly classification complexity. In addition, some classes of ship targets are relatively similar whether in the main structure of the targets or the distribution of scattering points. To solve this problem, the maximum margin criterion (MMC) is an effective method for maximizing the class separability [19,20].

To extract effective features of ship target from sea clutter and to ensure that the feature vector has high distinguishability, a method termed multi-scale fusion kernel SPP (MSFKSPP) based on the MMC is proposed. Here, a two-step strategy is taken. First of all, the multi-scale fusion kernel sparse reconstructive relationship is established. In the second, an optimal projection direction is automatically learned based on the MSFKSPP-MMC. Experiments on measured data show that the proposed method can effectively extract features of ship targets from sea clutter, reduce the feature dimensionality and improve the target recognition performance.

The major contributions of this paper can be summarized as follows.

(i) In the proposed method, the multi-scale fusion kernel sparse reconstructive relationship is constructed by combining the HRRPs under different scales and performing the kernel sparse preserving projection. The sparse reconstructive relationship can extract richer feature information of ship targets from sea clutter to avoid information loss and reduce the dimensionality.

(ii) The proposed method can maximally preserve the multi-scale fusion sparse reconstruct of data and maximize the class by separability resorting to the thought of MMC.

(iii) A novel framework, MSFKSPP-MMC, is mainly constructed for ship target recognition from the sea clutter. Consequently, the proposed method can make full use of data information and simultaneously utilize the label information of the target to improve the accuracy of HRRP recognition.

The remainder of this paper is organized as follows. In Section 2, the mechanism analysis of multi-scale features and dimension reduction is given. In Section 3, the HRRP RATR procedures via MSFKSPP-MMC are discussed in detail. The experimental results of HRRP target recognition are presented in Section 4. Finally, conclusions are drawn in Section 5.

2. Multi-scale features and dimension reduction mechanism analysis

2.1 Multi-scale features of HRRP

According to the scale-space theory [21,22], the multi-scale representation of HRRP is achieved by uniformly sampling the signal under continuous scale factors. Since the sampling vector $I(u)$ of HRRP is a one-dimensional signal, its multi-scale extraction is

$$L(u,\sigma) = \mathrm{LOG}(u,\sigma) \otimes I(u) \tag{1}$$

where $\otimes$ is the convolution operator, u is the spatial coordinate of HRRP cells, σ is the scale factor, and $\mathrm{LOG}(u,\sigma)$ is Laplace of Gaussian (LOG) kernel, which well preserves the peak and tough features of the dominant scatters. The definition of LOG kernel is

$$\mathrm{LOG}(u,\sigma) = \frac{u^2 - 2\sigma^2}{\sigma^4} \exp\left(-\frac{u^2}{2\sigma^2}\right). \tag{2}$$

So multi-scale features of an HRRP can be achieved by adjusting the parameter σ.

Fig. 1 shows an HRRP's multi-scale features of ship target with LOG kernel. From Fig. 1, it can be found that the positions and amplitude trends of the strong scatters do not have the apparent variations with the change of scale factor. At small-scale, the features of HRRP including the complete edge information can be extracted from the sea clutter. With the rising scale factor, the weak scatter is gradually submerged in the sea clutter, which makes the edge characteristics of the target change. It can be seen that small-scale features are prominent in local and

detail information, while the global and contour information is better in large-scale features. The most apparent changes among scales reflect on edge features. Since edges represent high frequency features, it can be seen that most of the information loss due to scaling factor rises comes from edge features. Multi-scale features help to extract the edge points of HRRPs from sea clutter. In this paper, aiming to extract richer feature information of ship target from sea clutter, we develop a sparse reconstruction relation with more discriminant information by using features at different scales.

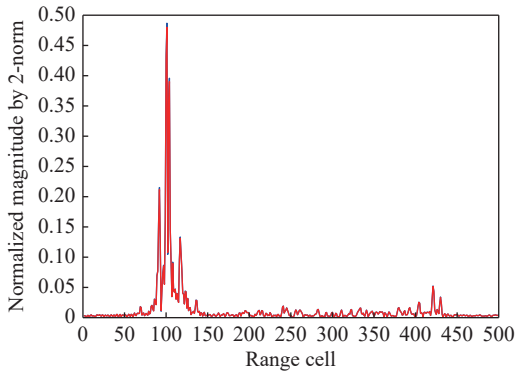

(a) Multi-scale range profile feature by scale factor σ=0.5

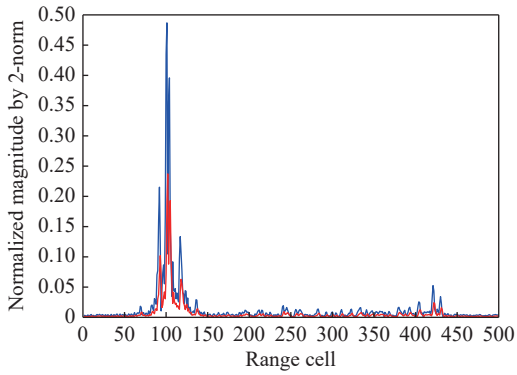

(b) Multi-scale range profile feature by scale factor σ=1.0

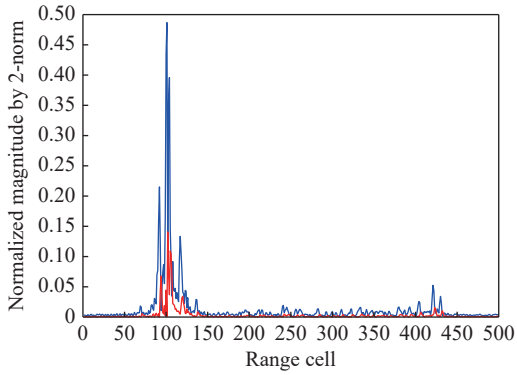

(c) Multi-scale range profile feature by scale factor σ=1.5

——: Original HRRP; ——: Multi-scale feature of HRRP.

Fig. 1 Multi-scale range profile features using LOG kernel

2.2 Dimensionality reduction based on SPP

Compared with air targets, the dynamic range of ship target length is larger. Reflected by the HRRPs, the proportion of the range units occupied by the range profile of the ship target in the wideband gate varies greatly. In engineering applications, stable tracking of the target is required before imaging and identification of the target. When imaging a target, we usually use the predicted position of the target as the center of the wideband gate for imaging. Due to radar system errors, data processing prediction errors, and other reasons, a larger wideband gate is required to ensure that the echo contains the complete range profile of the ship target. In this wideband gate, in addition to the range profile of the target, there is also a large amount of sea clutter, and the range profile of the target occupies only a small part of the wideband gate. A large amount of sea clutter increases the computational complexity and burdens the classifier. Therefore, it is necessary to reduce the dimensionality of HRRP of the ship target.

SPP [11,23,24] is a dimensionality reduction algorithm aiming to preserve the sparse reconstruction relationship of the data set. Assuming that C is the number of training HRRP classes, each class is composed of N_k $(k=1,2,\cdots,C)$ training HRRP samples, and $N=\sum_{k=1}^{C}N_k$ indicates the number of all training HRRP samples. $\boldsymbol{X}_k=[\boldsymbol{x}_{k,1},\boldsymbol{x}_{k,2},\cdots,\boldsymbol{x}_{k,l_k},\cdots,\boldsymbol{x}_{k,N_k}]\in\mathbf{R}^{n\times N_k}$ is the training HRRP samples matrix of the kth class, where $\boldsymbol{x}_{k,l_k}\in\mathbf{R}^n$ is a column vector of the l_kth HRRP sample in the kth class and n is the dimension of HRRP. $\boldsymbol{X}=[\boldsymbol{X}_1,\boldsymbol{X}_2,\cdots,\boldsymbol{X}_C]\in\mathbf{R}^{n\times N}$ is all training HRRP samples matrix. Each $\boldsymbol{x}_{k,l_k}$ can be sparsely represented by the rest of HRRP by solving the following optimization problem:

$$\boldsymbol{h}_{k,l_k}=\arg\min_{h_{k,l_k}}\left\|\boldsymbol{h}_{k,l_k}\right\|_1$$
$$\text{s.t.}\begin{cases}\boldsymbol{x}_{k,l_k}=\boldsymbol{X}\boldsymbol{h}_{k,l_k}\\ \boldsymbol{e}^{\mathrm{T}}\boldsymbol{h}_{k,l_k}=1\end{cases}\tag{3}$$

where $\boldsymbol{h}_{k,l_k}=[h_{k,l_k1,1},\cdots,h_{k,l_kk,l_{k-1}},0,h_{k,l_kk,l_{k+1}},\cdots,h_{k,l_kC,N_C}]^{\mathrm{T}}$ is the sparse representation coefficient vector, where the kl_kth element 0 represents that the sparse representation problem has nothing to do with $\boldsymbol{x}_{k,l_k}$ itself, and $\boldsymbol{e}$ represents the column vector where all elements are 1. In the case of noise, (3) can be represented as

$$\boldsymbol{h}_{k,l_k}=\arg\min_{h_i}\left\|\boldsymbol{h}_{k,l_k}\right\|_1$$
$$\text{s.t.}\begin{cases}\left\|\boldsymbol{X}\boldsymbol{h}_{k,l_k}-\boldsymbol{x}_{k,l_k}\right\|\leqslant\delta\\ \boldsymbol{e}^{\mathrm{T}}\boldsymbol{h}_{k,l_k}=1\end{cases}\tag{4}$$

where δ is the noise tolerance. Then SPP seeks a trans-

form matrix $\boldsymbol{V} \in \mathbf{R}^{n\times d}$ to project HRRP from a high-dimensional space into a d-dimensional space, where $n > d$ [23]. SPP aims to preserve the sparse reconstruction relationship and minimize the following objective function:

$$\min \sum_{k=1}^{C}\sum_{l_k=1}^{N_k}(\boldsymbol{V}^{\mathrm{T}}\boldsymbol{x}_{k,l_k}-\boldsymbol{V}^{\mathrm{T}}\boldsymbol{X}\boldsymbol{h}_{\boldsymbol{k},\boldsymbol{l_k}})^2 \quad \text{s.t. } \boldsymbol{V}^{\mathrm{T}}\boldsymbol{X}\boldsymbol{X}^{\mathrm{T}}\boldsymbol{V}=\boldsymbol{I} \tag{5}$$

where $\boldsymbol{I}$ is an identity matrix. Then, the optimization criteria of SPP method is obtained:

$$\min_{V}\frac{\boldsymbol{V}^{\mathrm{T}}\boldsymbol{X}(\boldsymbol{I}-\boldsymbol{H}-\boldsymbol{H}^{\mathrm{T}}+\boldsymbol{H}\boldsymbol{H}^{\mathrm{T}})\boldsymbol{X}^{\mathrm{T}}\boldsymbol{V}}{\boldsymbol{V}^{\mathrm{T}}\boldsymbol{X}\boldsymbol{X}^{\mathrm{T}}\boldsymbol{V}}. \tag{6}$$

Finally, the projection matrix $\boldsymbol{V}$ of SPP is the eigenvectors corresponding to smallest d eigenvalues which is obtained by

$$\boldsymbol{X}(\boldsymbol{I}-\boldsymbol{H}-\boldsymbol{H}^{\mathrm{T}}+\boldsymbol{H}\boldsymbol{H}^{\mathrm{T}})\boldsymbol{X}^{\mathrm{T}}\boldsymbol{V}=\lambda\boldsymbol{X}\boldsymbol{X}^{\mathrm{T}}\boldsymbol{V}. \tag{7}$$

The original high-dimensional HRRP can be projected into low-dimensional space through $\boldsymbol{V}$ to achieve the purpose of HRRP dimension reduction.

3. Ship target recognition base on HRRP via MSFKSPP-MMC

3.1 Principles of MSFKSPP

SPP is a linear dimensionality reduction algorithm. However, HRRPs of ship target are a type of highly nonlinear data set. In this subsection, in order to extract more distinguishable features of the target from sea clutter, we establish the kernel sparse reconstructive relationship under the constraints of multi-scale fusion and kernel sparsity preserving projection.

For a HRRP training sample $\boldsymbol{x}_{k,l_k} \in \mathbf{R}^n$, we transform it to different scale spaces and receive

$$\boldsymbol{z}_{k,l_k}^{\sigma_s}(u)=\mathrm{LOG}(u,\sigma_s)\otimes\boldsymbol{x}_{k,l_k}(u)\in\mathbf{R}^n$$

where σ_s is enumerated in the scale factor set:

$$\sum=\{\sigma_1,\sigma_2,\cdots,\sigma_s,\cdots,\sigma_S\},\ \ s=1,2,\cdots,S$$

where S is the total number of all scale factors. This paper sets the scale factor range between 0.5 and 10 with an interval of 0.5.

$\boldsymbol{Z}=[\boldsymbol{Z}_1^{s_1},\boldsymbol{Z}_1^{s_2},\cdots,\boldsymbol{Z}_1^{s_s},\cdots,\boldsymbol{Z}_1^{s_S},\cdots,\boldsymbol{Z}_k^{s_1},\boldsymbol{Z}_k^{s_2},\cdots,\boldsymbol{Z}_k^{s_s},\cdots,\boldsymbol{Z}_k^{s_S},\cdots,\boldsymbol{Z}_C^{s_1},\boldsymbol{Z}_C^{s_2}\cdots,\boldsymbol{Z}_C^{s_s},\cdots,\boldsymbol{Z}_C^{s_S}]$ is multi-scale transform matrix of HRRP training samples of all S scales, where $\boldsymbol{Z}_k^{s_s}=[\boldsymbol{z}_{k,1}^{\sigma_s},\boldsymbol{z}_{k,2}^{\sigma_s},\cdots,\boldsymbol{z}_{k,l_k}^{\sigma_s},\cdots,\boldsymbol{z}_{k,N_k}^{\sigma_s}]\in\mathbf{R}^{n\times N_k}$ is the scale training samples matrix of the kth class at σ_s scale. In view of the nonlinear characteristics hidden in HRRP, $\boldsymbol{z}_{k,l_k}^{\sigma_s}$ can be projected to a higher dimensional feature space $\boldsymbol{H}$ by a mapping function:

$$\phi:\boldsymbol{z}_{k,l_k}^{\sigma_s}\in\mathbf{R}^n\to\phi(\boldsymbol{z}_{k,l_k}^{\sigma_s})\in\boldsymbol{H}$$

$\boldsymbol{H}$ denotes a certain high dimensional feature space, where the inner product can be expressed as

$$K_{i,j}=K(\boldsymbol{z}_{i,l_{k1}}^{\sigma_{s1}},\boldsymbol{z}_{j,l_{k2}}^{\sigma_{s2}})=\left\langle\phi(\boldsymbol{z}_{i,l_{k1}}^{\sigma_{s1}}),\phi(\boldsymbol{z}_{j,l_{k2}}^{\sigma_{s2}})\right\rangle. \tag{8}$$

For any sample $\phi(\boldsymbol{z}_{k,l_k}^{\sigma_s})$, it can be analytically represented by all training samples except itself. Referring to SPP method, we can obtain the sparse vector $\hat{\boldsymbol{s}}_{k,i}^{s_s}$ by solving the following optimization problem:

$$\hat{\boldsymbol{s}}_{\boldsymbol{k},\boldsymbol{i}}^{s_s}=\arg\min_{s_{k,i}^{\sigma_s}}\left\|\boldsymbol{s}_{k,i}^{s_s}\right\|_1 \quad \text{s.t.}\begin{cases}\phi(\boldsymbol{z}_{k,l_k}^{\sigma_s})=\boldsymbol{B}\boldsymbol{s}_{k,i}^{s_s}\\ \boldsymbol{e}^{\mathrm{T}}\boldsymbol{s}_{k,i}^{s_s}=1\end{cases} \tag{9}$$

where $\boldsymbol{B}=[\phi(\boldsymbol{z}_{1,1}^{\sigma_1}),\phi(\boldsymbol{z}_{1,2}^{\sigma_1}),\cdots,\phi(\boldsymbol{z}_{1,N_1}^{\sigma_1}),\cdots,\phi(\boldsymbol{z}_{k,1}^{\sigma_s}),\phi(\boldsymbol{z}_{k,2}^{\sigma_s}),\cdots,\phi(\boldsymbol{z}_{k,N_k}^{\sigma_s}),\cdots,\phi(\boldsymbol{z}_{C,1}^{\sigma_S}),\phi(\boldsymbol{z}_{C,2}^{\sigma_S}),\cdots,\phi(\boldsymbol{z}_{C,N_C}^{\sigma_S})]$ is the matrix composed of all scale training samples in the high-dimensional feature space, $\boldsymbol{s}_{k,i}^{s_s}=[s_{k,i,\sigma_1,1,1}^{\sigma_s},\cdots,s_{k,i,\sigma_s,k,1}^{\sigma_s},\cdots,s_{k,i,\sigma_s,k,k-1}^{\sigma_s},0,s_{k,i,\sigma_s,k,k+1}^{\sigma_s},\cdots,s_{k,i,\sigma_s,C,1}^{\sigma_s},\cdots,s_{k,i,\sigma_S,C,N_C}^{\sigma_s}]^{\mathrm{T}}$ is a vector of multi-scale fusion kernel sparsity representation coefficients. Due to the presence of noise and the error of sample observations, $\phi(\boldsymbol{z}_{k,l_k}^{\sigma_s})=\boldsymbol{B}\boldsymbol{s}_{k,i}^{s_s}$ may not be sure to be always completely established [25], then (9) can be represented as

$$\hat{\boldsymbol{s}}_{k,i}^{s_s}=\arg\min_{s_{k,i}^{\sigma_s}}\left\|\boldsymbol{s}_{\boldsymbol{k},\boldsymbol{i}}^{s_s}\right\|_1 \quad \text{s.t.}\begin{cases}\left\|\boldsymbol{B}\boldsymbol{s}_{k,i}^{s_s}-\phi(\boldsymbol{z}_{k,l_k}^{\sigma_s})\right\|\leqslant\varepsilon\\ \boldsymbol{e}^{\mathrm{T}}\boldsymbol{s}_{k,i}^{s_s}=1\end{cases} \tag{10}$$

where ε is the noise tolerance. If ε in (10) is set to be 0, the optimization problem in (9) is equivalent to the optimization problem in (10). Therefore, the optimization problem in (9) can be regarded as a special case of optimization problem in (10), then only optimization problem in (10) need be considered. Since the exact expression of the nonlinear mapping ϕ is unknown, $\boldsymbol{B}$ and $\phi(\boldsymbol{z}_{k,l_k}^{\sigma_s})$ are also unknown, optimization problem in (10) cannot be solved directly. The optimization problem in (10) can be transformed into the following constrained optimization problem:

$$\hat{\boldsymbol{s}}_{\boldsymbol{k},\boldsymbol{i}}^{s_s}=\arg\min_{s_{k,i}^{\sigma_s}}\left\|\boldsymbol{s}_{k,i}^{s_s}\right\|_1 \quad \text{s.t.}\begin{cases}\left\|\boldsymbol{B}^{\mathrm{T}}\boldsymbol{B}\boldsymbol{s}_{\boldsymbol{k},\boldsymbol{i}}^{s_s}-\boldsymbol{B}^{\mathrm{T}}\phi(\boldsymbol{z}_{k,l_k}^{\sigma_s})\right\|\leqslant\delta\\ \boldsymbol{e}^{\mathrm{T}}\boldsymbol{s}_{k,i}^{s_s}=1\end{cases}. \tag{11}$$

Using the kernel function to calculate inner product of high dimensional feature space data, we can obtain

$$\boldsymbol{B}^{\mathrm{T}}\boldsymbol{B}=\begin{bmatrix} K(z_{1,1}^{\sigma_1},z_{1,1}^{\sigma_1}) & K(z_{1,1}^{\sigma_1},z_{1,2}^{\sigma_1}) & \cdots & K(z_{1,1}^{\sigma_1},z_{C,N_C}^{\sigma_S}) \\ K(z_{1,2}^{\sigma_1},z_{1,1}^{\sigma_1}) & K(z_{1,2}^{\sigma_1},z_{1,2}^{\sigma_1}) & \cdots & K(z_{1,2}^{\sigma_1},z_{C,N_C}^{\sigma_S}) \\ \vdots & \vdots & \ddots & \vdots \\ K(z_{C,N_C}^{\sigma_S},z_{1,1}^{\sigma_1}) & K(z_{C,N_C}^{\sigma_S},z_{1,2}^{\sigma_1}) & \cdots & K(z_{C,N_C}^{\sigma_S},z_{C,N_C}^{\sigma_S}) \end{bmatrix}=\boldsymbol{K},\ \boldsymbol{B}^{\mathrm{T}}\phi(z_{k,l_k}^{\sigma_s})=\begin{bmatrix} K(z_{1,1}^{\sigma_1},z_{k,l_k}^{\sigma_s}) \\ K(z_{1,2}^{\sigma_1},z_{k,l_k}^{\sigma_s}) \\ \vdots \\ K(z_{C,N_C}^{\sigma_S},z_{k,l_k}^{\sigma_s}) \end{bmatrix}.$$

The multi-scale fusion kernel sparsity representation coefficients $\hat{\boldsymbol{s}}_{k,i}^{s_s}$ can be obtained by solving (11). In addition, the multi-scale fusion kernel sparse reconstructive weight matrix $\boldsymbol{S}\in\mathbf{R}^{SN\times SN}$ can be defined as follows:

$$\boldsymbol{S}=[\hat{\boldsymbol{s}}_{1,1}^{s_1},\hat{\boldsymbol{s}}_{1,2}^{s_1},\cdots,\hat{\boldsymbol{s}}_{1,N_1}^{s_s},\cdots,\hat{\boldsymbol{s}}_{k,N_k}^{s_s},\cdots,\hat{\boldsymbol{s}}_{C,1}^{s_1},\cdots,\hat{\boldsymbol{s}}_{C,N_C,}^{s_s},\cdots,\hat{\boldsymbol{s}}_{C,N_C}^{s_S}].$$

Note that the relationship between samples of different scale spaces is achieved, which can improve the accuracy of target recognition. Then we can seek the projections of multi-scale fusion kernel sparsity preserves projection by solving the following function:

$$\min\sum_{s=1}^{S}\sum_{k=1}^{C}\sum_{l_k=1}^{N_k}(\boldsymbol{V}^{\mathrm{T}}\phi(z_{k,l_k}^{\sigma_s})-\boldsymbol{V}^{\mathrm{T}}\boldsymbol{B}\hat{\boldsymbol{s}}_{\boldsymbol{k,i}}^{s_s})^2 \tag{12}$$

with

$$\sum_{s=1}^{S}\sum_{k=1}^{C}\sum_{i=1}^{N_k}(\boldsymbol{V}^{\mathrm{T}}\phi(z_{k,i}^{\sigma_s})-\boldsymbol{V}^{\mathrm{T}}\boldsymbol{B}\hat{\boldsymbol{s}}_{k,i}^{\sigma_s})^2=$$
$$\boldsymbol{V}^{\mathrm{T}}\boldsymbol{B}(\sum_{s=1}^{S}\sum_{k=1}^{C}\sum_{i=1}^{N_k}(e_{k,i}^{\sigma_s}-\hat{\boldsymbol{s}}_{k,i}^{\sigma_s})(e_{k,i}^{\sigma_s}-\hat{\boldsymbol{s}}_{k,i}^{\sigma_s})^{\mathrm{T}})\boldsymbol{B}^{\mathrm{T}}\boldsymbol{V}=$$
$$\boldsymbol{V}^{\mathrm{T}}\boldsymbol{B}(\boldsymbol{I}-\boldsymbol{S}-\boldsymbol{S}^{\mathrm{T}}+\boldsymbol{S}\boldsymbol{S}^{\mathrm{T}})\boldsymbol{B}^{\mathrm{T}}\boldsymbol{V}=\boldsymbol{V}^{\mathrm{T}}\boldsymbol{B}\boldsymbol{L}\boldsymbol{B}^{\mathrm{T}}\boldsymbol{V} \tag{13}$$

where $\boldsymbol{L}=\boldsymbol{I}-\boldsymbol{S}-\boldsymbol{S}^{\mathrm{T}}+\boldsymbol{S}\boldsymbol{S}^{\mathrm{T}}$, and $\boldsymbol{e}_{k,i}^{s_s}$ is an SN-dimensional column vector in which the skith element is equal to 1 and the rest of elements are all equal to 0. We can obtain the following optimization problem:

$$\min\sum_{s=1}^{S}\sum_{k=1}^{C}\sum_{l_k=1}^{N_k}(\boldsymbol{V}^{\mathrm{T}}\phi(z_{k,l_k}^{\sigma_s})-\boldsymbol{V}^{\mathrm{T}}\boldsymbol{B}\hat{\boldsymbol{s}}_{k,i}^{s_s})^2=$$
$$\min\ \boldsymbol{V}^{\mathrm{T}}\boldsymbol{B}\boldsymbol{L}\boldsymbol{B}^{\mathrm{T}}\boldsymbol{V}=\min\ \boldsymbol{Y}\boldsymbol{L}\boldsymbol{Y}^{\mathrm{T}} \tag{14}$$

where $\boldsymbol{Y}=\boldsymbol{V}^{\mathrm{T}}\boldsymbol{B}$ and $\boldsymbol{L}=\boldsymbol{I}-\boldsymbol{S}-\boldsymbol{S}^{\mathrm{T}}+\boldsymbol{S}\boldsymbol{S}^{\mathrm{T}}=\boldsymbol{L}^{\mathrm{T}}$. So $\boldsymbol{Y}\boldsymbol{L}\boldsymbol{Y}^{\mathrm{T}}$ is a quadratic matrix, then we can obtain the following optimization problem:

$$\min\sum_{s=1}^{S}\sum_{k=1}^{C}\sum_{l_k=1}^{N_k}(\boldsymbol{V}^{\mathrm{T}}\phi(z_{k,l_k}^{\sigma_s})-\boldsymbol{V}^{\mathrm{T}}\boldsymbol{B}\hat{\boldsymbol{s}}_{\boldsymbol{k,i}}^{s_s})^2=$$
$$\min\ \mathrm{tr}[\boldsymbol{V}^{\mathrm{T}}\boldsymbol{B}\boldsymbol{L}\boldsymbol{B}^{\mathrm{T}}\boldsymbol{V}]. \tag{15}$$

To avoid the divergence of the solution, a constraint $\boldsymbol{V}^{\mathrm{T}}\boldsymbol{B}\boldsymbol{B}^{\mathrm{T}}\boldsymbol{V}=\boldsymbol{I}$ is imposed on (15).

According to the regenerative nucleus theory, in (15), $\boldsymbol{V}$ can be written as $\boldsymbol{V}=\boldsymbol{B}\boldsymbol{a}$, where $\boldsymbol{a}=[\alpha_{1,1}^{\sigma_1},\alpha_{1,2}^{\sigma_1},\cdots,\alpha_{1,N_1}^{\sigma_1},\cdots,\alpha_{k,N_k}^{\sigma_s},\cdots,\alpha_{C,N_C}^{\sigma_S}]^{\mathrm{T}}$ is to be determined. Substituting $\boldsymbol{V}=\boldsymbol{B}\boldsymbol{a}$ into (15), we can obtain the following optimization problem:

$$\min\sum_{s=1}^{S}\sum_{k=1}^{C}\sum_{l_k=1}^{N_k}(\boldsymbol{V}^{\mathrm{T}}\phi(z_{k,l_k}^{\sigma_s})-\boldsymbol{V}^{\mathrm{T}}\boldsymbol{B}\hat{\boldsymbol{s}}_{k,i}^{s_s})^2=$$
$$\min\ \mathrm{tr}[\boldsymbol{a}^{\mathrm{T}}\boldsymbol{K}\boldsymbol{L}\boldsymbol{K}\boldsymbol{a}]$$
$$\text{s.t. }\boldsymbol{a}^{\mathrm{T}}\boldsymbol{K}^2\boldsymbol{a}=\boldsymbol{I}. \tag{16}$$

MSFKSPP can maximally preserve the sparse reconstructive of data without discrimination. On the other hand, between certain classes of ship targets, there is little difference in target shape, structure, or size. MMC can reduce the within-class dispersion, increase the between-class dispersion and improve the recognition ability.

3.2 Ship target recognition method based on MSFKSPP-MMC

To maximally preserve the structure of the data in the dimension-reduced space and improve the classification performance simultaneously, the merits of MSFKSPP and MMC are fused. In this subsection, we learn an optimal projection direction automatically based on the MSFKSPP-MMC. The optimal projection direction makes full use of data information and labels information.

Similar to MSFKSPP method, kernel MMC aims to find the optimal projection direction $\boldsymbol{V}$ to maximize the margin between interclass samples. The objective function can be expressed as follows [19,26]:

$$\max\ \mathrm{tr}[\boldsymbol{V}^{\mathrm{T}}(\boldsymbol{S}_b^{\phi}-\boldsymbol{S}_{\omega}^{\phi})\boldsymbol{V}]=$$
$$\max\ \mathrm{tr}[\boldsymbol{a}^{\mathrm{T}}\boldsymbol{B}^{\mathrm{T}}\boldsymbol{B}(\boldsymbol{S}_1-\mu\boldsymbol{S}_2)\boldsymbol{B}^{\mathrm{T}}\boldsymbol{B}\boldsymbol{a}]=$$
$$\max\ \mathrm{tr}[\boldsymbol{a}^{\mathrm{T}}\boldsymbol{K}(\boldsymbol{S}_1-\mu\boldsymbol{S}_2)\boldsymbol{K}\boldsymbol{a}] \tag{17}$$

where $\boldsymbol{S}_b^{\phi}$ and $\boldsymbol{S}_{\omega}^{\phi}$ are the between-class scatter matrix and within-class scatter matrix, respectively.

$$\boldsymbol{S}_b^{\phi}=\frac{1}{NS}\sum_{k=1}^{C}N_kS\,(\boldsymbol{m}_k^{\phi}-\boldsymbol{m}^{\phi})(\boldsymbol{m}_k^{\phi}-\boldsymbol{m}^{\phi})^{\mathrm{T}},$$

$$\boldsymbol{S}_{\omega}^{\phi}=\frac{1}{NS}\sum_{k=1}^{C}\boldsymbol{S}_k^{\phi},$$

and

$$\boldsymbol{S}_k^{\phi}=\sum_{s=1}^{S}\sum_{i=1}^{N_k}[\phi(z_{k,i}^{\sigma_s})-\boldsymbol{m}_k^{\phi}][\phi(z_{k,i}^{\sigma_s})-\boldsymbol{m}_k^{\phi}]^{\mathrm{T}}\boldsymbol{m}_k^{\phi}=$$
$$\frac{1}{N_kS}\sum_{s=1}^{S}\sum_{i=1}^{N_k}\phi(z_{k,i}^{\sigma_s})\boldsymbol{m}^{\phi}=\frac{1}{C}\sum_{k=1}^{C}\boldsymbol{m}_k^{\phi},$$

$$\boldsymbol{S}_2 = \frac{1}{NS}[\boldsymbol{I} - \frac{1}{N_k S}\sum_{k=1}^{C}\sum_{s=1}^{S}\boldsymbol{e}_{s_s}{}^{c}(\boldsymbol{e}_{s_s}{}^{c})^{\mathrm{T}}],$$

$$\boldsymbol{S}_t = \frac{1}{NS}[\boldsymbol{I} - \frac{\boldsymbol{e}\boldsymbol{e}^{\mathrm{T}}}{NS}],$$

$$\boldsymbol{S}_1 = \boldsymbol{S}_t - \boldsymbol{S}_2,$$

where μ is positive constant, $\boldsymbol{e}$ is an NS-dimensional unit vector, $\boldsymbol{e}_c^c$ is an NS-dimensional vector with $e_{\sigma_s}^c(k) = 1$ and $e_{\sigma_s}^c(i) = 0$ $(i = 1, 2, \cdots, NS$ when $i \neq k)$.

By combining (16) and (17), we can get the following optimization problem:

$$\begin{cases} \min\ \mathrm{tr}[\boldsymbol{a}^{\mathrm{T}}\boldsymbol{K}\boldsymbol{L}\boldsymbol{K}\boldsymbol{a}] \\ \max\ \mathrm{tr}[\boldsymbol{a}^{\mathrm{T}}\boldsymbol{K}(\boldsymbol{S}_1 - \mu\boldsymbol{S}_2)\boldsymbol{K}\boldsymbol{a}] \\ \text{s.t. } \boldsymbol{a}^{\mathrm{T}}\boldsymbol{K}^2\boldsymbol{a} = \boldsymbol{I}. \end{cases} \tag{18}$$

The solution to the multi-objective constrained optimization problem in (18) is to find a subspace which preserves the sparsity property and maximizes the margin between different classes simultaneously. Therefore we can change (18) into the following constrained problem:

$$\begin{aligned} &\max\ \mathrm{tr}[\boldsymbol{V}^{\mathrm{T}}(\boldsymbol{S}_b^{\phi} - \boldsymbol{S}_{\omega}^{\phi})\boldsymbol{V}] - \eta\mathrm{tr}[\boldsymbol{V}^{\mathrm{T}}\boldsymbol{B}\boldsymbol{L}\boldsymbol{B}^{\mathrm{T}}\boldsymbol{V}] = \\ &\quad \mathrm{tr}[\boldsymbol{a}^{\mathrm{T}}\boldsymbol{B}^{\mathrm{T}}\boldsymbol{B}(\boldsymbol{S}_1 - \mu\boldsymbol{S}_2 - \eta\boldsymbol{L})\boldsymbol{B}^{\mathrm{T}}\boldsymbol{B}\boldsymbol{a}] = \\ &\quad\quad \mathrm{tr}[\boldsymbol{a}^{\mathrm{T}}\boldsymbol{K}(\boldsymbol{S}_1 - \mu\boldsymbol{S}_2 - \eta\boldsymbol{L})\boldsymbol{K}\boldsymbol{a}] \\ &\quad\quad\quad \text{s.t. } \boldsymbol{a}^{\mathrm{T}}\boldsymbol{K}^2\boldsymbol{a} = \boldsymbol{I} \end{aligned} \tag{19}$$

where $\boldsymbol{K}$ is the basic kernel, and η is a positive constant to adjust the effects of MSFKSPP structure information. (19) can be solved by Lagrange multiplier method:

$$\frac{\partial}{\partial \boldsymbol{a}}\mathrm{tr}[\boldsymbol{a}^{\mathrm{T}}\boldsymbol{K}(\boldsymbol{S}_1 - \mu\boldsymbol{S}_2 - \eta\boldsymbol{L})\boldsymbol{K}\boldsymbol{a}] - \lambda(\boldsymbol{a}^{\mathrm{T}}\boldsymbol{K}^2\boldsymbol{a} - \boldsymbol{I}) = 0$$

where λ is the Lagrange multiplier. The maximization criterion in (19) can be transformed into solving the following generalized eigenequation:

$$\boldsymbol{K}(\boldsymbol{S}_1 - \mu\boldsymbol{S}_2 - \eta\boldsymbol{L})\boldsymbol{K}\boldsymbol{a} = \lambda\boldsymbol{K}^2\boldsymbol{a}. \tag{20}$$

Finally, the projection matrix of the proposed method is the largest d eigenvalues of $\alpha_i (i = 1, 2, \cdots, d)$ which is obtained by (20). After the mapping matrix is obtained, both the training samples and the testing samples can be mapped into a low-dimensional feature space:

$$\boldsymbol{y}_{k,l_k} = \boldsymbol{V}^{\mathrm{T}}\phi(\boldsymbol{x}_{k,l_k}) = \boldsymbol{a}^{\mathrm{T}}\boldsymbol{B}^{\mathrm{T}}\phi(\boldsymbol{x}_{k,l_k}) = \boldsymbol{a}^{\mathrm{T}}\begin{bmatrix} K(\boldsymbol{z}_{1,1}^{\sigma_1}, \boldsymbol{x}_{k,l_k}) \\ K(\boldsymbol{z}_{1,2}^{\sigma_1}, \boldsymbol{x}_{k,l_k}) \\ \vdots \\ K(\boldsymbol{z}_{C,N_C}^{\sigma_S}, \boldsymbol{x}_{k,l_k}) \end{bmatrix},$$

$$\boldsymbol{y}'_{q,l_k} = \boldsymbol{V}^{\mathrm{T}}\phi(\boldsymbol{x}'_{q,l_k}) = \boldsymbol{a}^{\mathrm{T}}\boldsymbol{B}^{\mathrm{T}}\phi(\boldsymbol{x}'_{q,l_k}) = \boldsymbol{a}^{\mathrm{T}}\begin{bmatrix} K(\boldsymbol{z}_{1,1}^{\sigma_1}, \boldsymbol{x}'_{q,l_k}) \\ K(\boldsymbol{z}_{1,2}^{\sigma_1}, \boldsymbol{x}'_{q,l_k}) \\ \vdots \\ K(\boldsymbol{z}_{C,N_C}^{\sigma_S}, \boldsymbol{x}'_{q,l_k}) \end{bmatrix},$$

where $\boldsymbol{x}'_{q,l_k}$ denotes a testing sample $(q = 1, 2, \cdots, p)$. p is the number of testing classes. After feature extraction, the testing samples and training samples are recorded as $\boldsymbol{Y}' = \{\boldsymbol{y}'_{1,1}, \boldsymbol{y}'_{2,3}, \cdots, \boldsymbol{y}'_{q,l_k}, \cdots, \boldsymbol{y}'_{p,N_p}\}$ and $\boldsymbol{Y} = \{\boldsymbol{y}_{1,1}, \boldsymbol{y}_{2,2}, \cdots, \boldsymbol{y}_{k,l_k}, \cdots, \boldsymbol{y}_{C,N_C}\}$ respectively. In this paper, the support vector machine (SVM) classifier is adopted in the testing stage.

The whole procedure of performing classification by MSFKSPP-MMC can be formally summarized as follows.

Input Train data matrix $\boldsymbol{X} = [\boldsymbol{X}_1, \boldsymbol{X}_2, \cdots, \boldsymbol{X}_C]$ and the corresponding labels C; testing data $\boldsymbol{X}'$.

Step 1 Transform the training sample matrix $\boldsymbol{X}$ into the multi-scale transform matrix $\boldsymbol{Z}$ by multi-scale extraction.

Step 2 Obtain the optimizer $\hat{\boldsymbol{s}}_{\boldsymbol{k},\boldsymbol{i}}^{s_s}$ to problem in (11) and calculate the multi-scale fusion kernel sparse reconstructive weight matrix $\boldsymbol{S}$.

Step 3 Obtain the optimizer $\boldsymbol{a}$ to problem (19) and compute the optimization projection matrix $\boldsymbol{V}$.

Step 4 Calculate the low-dimensional embedding $\boldsymbol{Y}$ for training data and $\boldsymbol{Y}'$ for testing data.

Step 5 Classify the testing data according to the SVM.

4. Experimental results and analyses

In this section, we present several experimental results demonstrating the effectiveness of the proposed method for classification tasks on measured datasets. We compare the results of our method with those of SPP [11], kernel SPP (KSPP) [27], multi-scale fusion SPP (MSPP) [28], and kernel PCA (KPCA) [29].

4.1 HRRP data set of ship targets

To verify the effectiveness and robustness of the proposed method, some vital experiments are carried out based on the measured data. The dataset is balanced and composed of four classes. The dataset is composed of real HRRPs generated by numerous homogeneous coastal surveillance radars, which is an S-band radar with the radar bandwidth of 300 MHz. Specially, each raw HRRP is a 2 048-dimensinal long vector. The labels of the data samples are derived from intelligence support and the labels are confirmed by the operator.

Generally, the antenna erection height of coastal surveillance radar ranges from tens of meters to more than one thousand meters above sea level, and the maximum detection distance is tens of kilometers. Ignoring the inclination of the ship caused by the waves, it can be calculated that the range of the radar grazing angle is approximately 0.5° to 5°. Relative to the azimuth angle that can be changed in the range of 0° to 360°, the influ-

ence of the change of the grazing angle is negligible. Therefore, this paper only considers the azimuth sensitivity. Here we define attitude angle, which is the included angle between radar line of sight and target heading, and its value ranges from 0° to 180°. When the attitude is greater than 70° or less than 110°, the sea surface ship target is in tangential or approximate a tangential motion state. At this time, HRRPs cannot completely represent the inherent structural characteristics of the target.

Therefore, HRRPs with the attitude range of 0°−70° and 110°−180° are selected for experimental analysis. The dataset is balanced and composed of four classes of range profiles. A characteristic example HRRP of each class can be seen in Fig. 2. A total of 1 200 HRRPs are available for each class. In order to reduce the impact of amplitude sensitivity on the recognition results, the HRRPs are normalized.

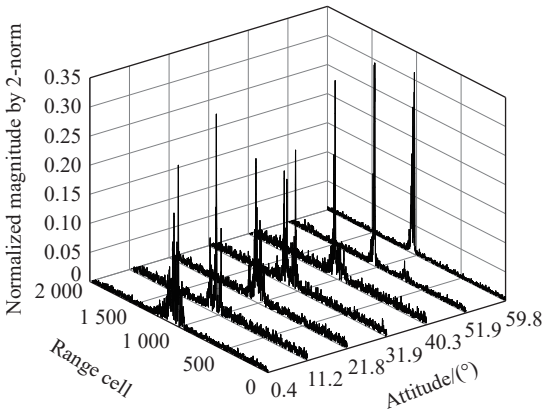

Fig. 2 Characteristic example HRRPs of ship target

In the following experiments, we will use Gaussian kernel

$$K_G(x,y)=\exp\left(-\frac{(x-y)^2}{c}\right)$$

where c is a constant parameter and is set to 5. The values of μ and η are jointly searched from [1e-4,1e-3,1e-2, 1e-1,1,1e1,1e2,1e3,1e4]. The number of HRRPs for training and testing is tabulated in Table 1.

Table 1 Number of HRRP for training and testing about the four classes targets

Target	Training sample	Testing sample
Class 1	700	500
Class 2	700	500
Class 3	700	500
Class 4	700	500

4.2 Influences of different number of scale factors

To verify the performance of the proposed method, the effects of different number of scale factors are discussed. In the comparison experiments, the number of scale factors is set as 1, 2, 3, 4, 5, 6, 7, 8, and 9, respectively. The value μ and η are equal to 1. The average recognition accuracy of four classes with different numbers of scale factors is shown in Fig. 3, which shows that the results obtained by different numbers of scale factors are significantly different. It means that multi-scale fusion kernel functions can effectively characterize the data in the reproducing kernel Hilbert space. We can see that the model has the different recognition ability under different numbers of scale factors, which indicates that the number of scale factors has a certain influence on the recognition accuracy.

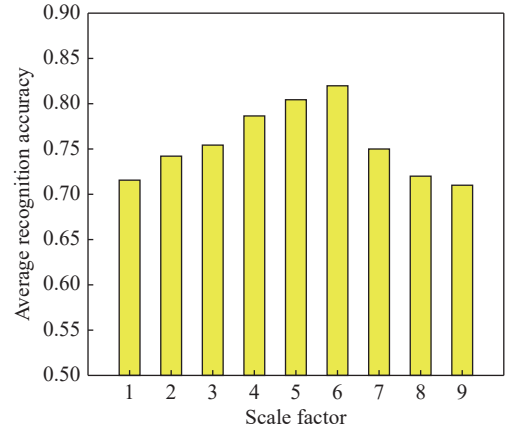

Fig. 3 Average recognition accuracy of four classes with different number of scale factors

The scale factor selection is an important issue in multi-scale technologies. The proper scale factors could greatly enhance the performance of multi-scale classification. This paper takes Kullback-Leibler divergence (KL-divergence) method to achieve the scale factor selection [30]. This paper sets the scale factor range between 0.5 and 10 with an interval of 0.5. The KL-divergence value with a different number of scale factors is shown in Fig. 4. Combining Fig. 3 and Fig. 4, it can be seen that the optimum number of scale factor is 6. In later experiments, we use the scale factor of 6 for analysis.

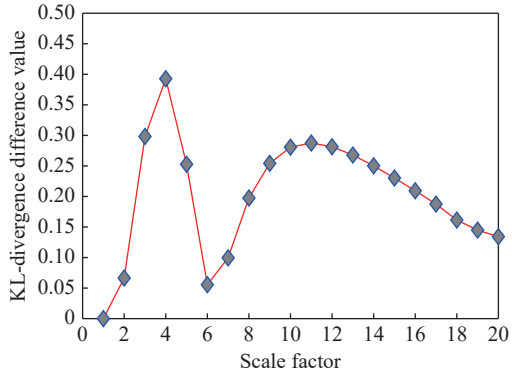

Fig. 4 KL-divergence difference value with different number of scale factors

4.3 Average recognition accuracy with different feature dimensions

In this subsection, we show the reduced feature dimension of the corresponding algorithms. Fig. 5 shows the average recognition accuracy of four classes with different feature dimensions. From the analysis, the average recognition accuracy of all methods improves with increasing feature dimensions. However, after a certain feature dimension, the average recognition accuracy performance remains almost unchanged. Compared with the corresponding algorithms, the feature dimension of projection vectors in the proposed method is the highest. This is because the proposed method deeply extracts feature information from the training sample. The best average recognition accuracy shows that the proposed method can effectively extract local and global information from sea clutter.

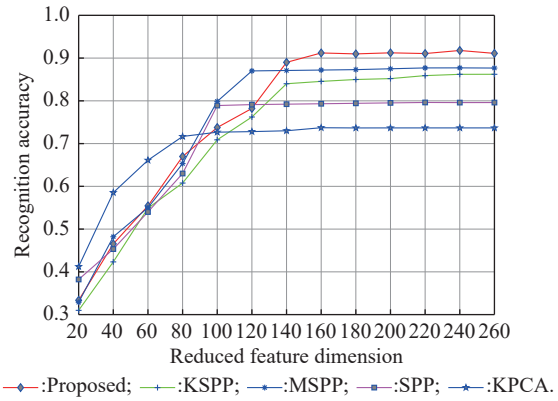

Fig. 5 Average recognition accuracy with different feature dimensions

4.4 Average recognition accuracy comparison versus different training sample sizes

To verify the proposed method can solve sample problems, we compare the performance of the proposed method with KSPP, MSPP, SPP, and KPCA under small training sample size. The training sample size which is tabulated in Table 1 is set as 20%, 40%, 60%, 80%, and 100% of the original training sample size, respectively, and then we use all of the testing sample size as testing sample size to evaluate performances. Experimental results are shown in Fig. 6.

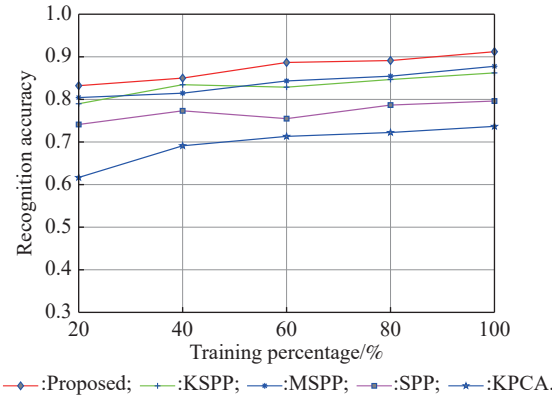

Fig. 6 Average recognition accuracy with different training sample sizes

As shown in Fig. 6, we can see that the recognition accuracies of all the methods declined with the number of training samples decreasing which conforms to the general law of model learning. For insufficient training sample sizes which lead to the small sample problem, the proposed method still achieves the best recognition performance. On the other hand, we find that some methods have better recognition accuracies with a small training sample size (40% for KSPP, and 40% for SPP) than those with a large training sample size (60% for KSPP, and 60% for SPP). This may be because the training sample is small, so the redundant information is removed and the effective information of the target is retained. When the training sample size increases to more than 60%, the recognition accuracies of all methods are increased. Among all the approaches, the proposed method has the ability to preserve the multi-scale fusion kernel sparsity preserves projection of the data, and maximize the distances between different classes, which achieved the highest recognition rate.

5. Conclusions

In this paper, the method via MSFKSPP-MMC is proposed for radar HRRP target recognition which is an efficient approach for dimensionality reduction and feature extraction. The kernel sparse reconstructive relationship of multi-scale fusion is constructed. The proposed method can extract richer feature information of ship targets from sea clutter, simultaneously preserve the multi-scale fusion kernel sparsity preserves projection of the data and maximize the class separability in the dimensionality reduced reproducing kernel Hilbert space. Extensive studies on the measured data demonstrate that the proposed method exhibits a good classification performance. Moreover, compared with other methods in HRRP target recognition, it shows the superiority of the proposed method.

References

[1] CHEN W C, CHEN B, PENG X J, et al. Tensor RNN with Bayesian nonparametric mixture for radar HRRP modeling and target recognition. IEEE Trans. on Signal Processing, 2021, 69(1): 1995–2009.

[2] PAN M A, LIU A L, YU Y Z, et al. Radar HRRP target recognition model based on a stacked CNN-Bi-RNN with attention mechanism. IEEE Trans. on Geoscience and Remote Sensing, 2022, 60(1): 5100814.

[3] SHI L C, LIANG Z H, ZHUANG Y, et al. One-shot HRRP generation for radar target recognition. IEEE Geoscience and Remote Sensing Letter, 2022, 19(1): 3504405.

[4] GUO P C, LIU Z, WANG J J. Radar group target recognition based on HRRPs and weighted mean shift clustering. Journal of Systems Engineering and Electronics, 2020, 31(6): 1152–1159.

[5] SHUI P L, ZHANG K. Ship radial size estimation in high-resolution maritime surveillance radars via sparse recovery using linear programming. IEEE Access, 2019, 7: 70673–70688.

[6] CHEN Y, WANG S H, CHEN W L, et al. A length and width feature extraction method of ship target based on IR image. Proc. of the 7th International Conference on Communications, Signal Processing, and Systems, 2018: 3−10.

[7] LIU J, FANG N, XIE Y X, et al. Multi-scale feature-based fuzzy-support vector machine classification using radar range profiles. IET Radar, Sonar and Navigation, 2016, 10(2): 370–378.

[8] WU H, DAI D H, WANG X S. A novel radar HRRP recognition method with accelerated T-distributed stochastic neighbor embedding and density-based clustering. Sensors, 2019, 19(23): 5112.

[9] LIU J, SU M, XU Q Y. Multi-scale feature vector reconstruction for aircraft classification using high range resolution radar signatures. Journal of Electromagnetic Waves and Applications, 2021, 35(14): 1843–1862.

[10] ZHANG H H, DING D Z, FAN Z H, et al. Adaptive neighborhood-preserving discriminant projection method for HRRP-based radar target recognition. IEEE Antennas and Wireless Propagation Letters, 2015, 14: 650–653.

[11] XU B Z, CHEN Y Q, GU H, et al. Multi-view features-based HRRP classification via sparsity preserving projection. Proc. of the 8th International Conference on Control, 2019. DOI: 10.1109/ICCAIS46528.2019.9074684.

[12] ZHANG A, GAO X W. Data-dependent kernel sparsity preserving projection and its application for semi-supervised classification. Multimedia Tools and Applications, 2018, 77(1): 24459–24475.

[13] REN H H, YU X L, WANG X G. Supervised kernel discriminant local tangent space alignment for high-resolution range profile-based radar target recognition. Journal of Applied Remote Sensing, 2020, 13(4): 046513.

[14] XIONG W, ZHANG G, LIU S, et al. Multiscale kernel sparse coding based classifier for HRRP radar target recognition. IET Radar, Sonar and Navigation, 2016, 10(9): 1594–1602.

[15] LIU W B, YUAN J W, ZHANG G. HRRP target recognition based on kernel joint discriminant analysis. Journal of Systems Engineering and Electronics, 2019, 30(4): 703–708.

[16] ZHOU D Y, SHEN X F, WANG G L, et al. Orthogonal kernel projecting plane for radar HRRP recognition. NeuroComputing, 2013, 106(1): 61–67.

[17] ZHANG K, SHUI P L. Estimation of complex high-resolution range profiles of ships by sparse recovery iterative minimization method. IEEE Trans. on Aerospace and Electronic Systems, 2021, 57(5): 3042–3056.

[18] LIU J, NING F, YONG J X, et al. Scale-space theory-based multi-scale feature for aircraft classification using HRRP. Electronics Letters, 2016, 52(6): 475–477.

[19] LI H F, JIANG T, ZHANG K S. Efficient and robust feature extraction by maximum margin criterion. IEEE Trans. on Neural Networks, 2006, 17(1): 157–165.

[20] ZHOU D Y. Orthogonal maximum margin projection subspace for radar target HRRP recognition. EURASIP Journal on Wireless Communications and Networking, 2016, 2016(1): 72.

[21] LINDEBERG T. Scale-space theory: a basic tool for analysing structures at different scales. Journal of Applied Statistics, 1994, 21(2): 224–270.

[22] GAO X Z, PENG X. Robust sequential high-resolution range profile recognition based on the infinite conditional restricted Boltzmann machine. IET Radar, Sonar and Navigation, 2020, 14(1): 71–80.

[23] QIAO L S, CHEN S C, TAN X Y. Sparsity preserving projections with applications to face recognition. Pattern Recognition, 2010, 43(1): 331–341.

[24] MIAO X Y, SHAN Y P. SAR target recognition via sparse representation of multi-view SAR images with correlation analysis. Journal of Electromagnetic Waves and Applications, 2019, 33(7): 897–910.

[25] YIN J, YANG W K. Kernel sparsity preserving projections and its application to biometrics. Acta Electronica Sinica, 2013, 41(4): 639–645.

[26] LI C, BAO W M, XU L P, et al. Multiple kernel learning via orthogonal neighborhood preserving projection and maximum margin criterion method for synthetic aperture radar target recognition. Optical Engineering, 2018, 57(5): 053105.

[27] ZHANG R, SUN Q. Canonical correlation analysis algorithm based on kernel sparsity preserve projection. Journal of Data Acquisition and Processing, 2017, 32(1): 111–118.

[28] DAI W L, ZHANG G, ZHANG Y. HRRP classification based on multi-scale fusion sparsity preserving projections. Electronics Letters, 2017, 53(11): 748–750.

[29] CHEN B, LIU H W, BAO Z. PCA and kernel PCA for radar high range resolution profiles recognition. Proc. of the IEEE Radar Conference, 2005: 528–533.

[30] WILCHER J S, LANTERMAN A D, MELVIN W L. Using an information-theoretic measure to inform distributed radar placement for automatic target recognition. IET Radar, Sonar and Navigation, 2016, 10(6): 1098–1106.

Biographies

YANG Xueling was born in 1986. He received his B.S. and M.S. degrees from the College of Mathematical Sciences, Harbin Engineering University, Heilongjiang, China, in 2008 and 2011, respectively. He is a Ph.D. candidate in Nanjing University of Aeronautics and Astronautics. He is a senior engineer with the Nanjing Marine Radar Institute. His current research interests are radar target recognition and radar signal processing.

E-mail: yangxueling@nuaa.edu.cn

ZHANG Gong was born in 1964. He received his Ph.D. degree from Nanjing University of Aeronautics and Astronautics (NUAA) in 2002. He is a professor in the College of Electronics and Information Engineering, NUAA. He is a member of the Committee of Electromagnetic Information, Chinese Society of Astronautics (CEI-CSA), and a senior member of the Chinese Institute of Electronics (CIE). His research interests are synthetic aperture rader (SAR) image processing, target detection, and target recognition.
E-mail: gzhang@nuaa.edu.cn

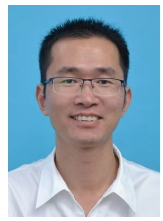

SONG Hu was born in 1980. He received his M.S. and Ph.D. degrees from the Communication System, Nanjing University of Science and Technology, Nanjing, China, in 2005 and 2020, respectively. He is a senior engineer with the Nanjing Marine Radar Institute. His current research interest is radar target recognition.
E-mail: andysonghu@126.com